

Chain-like ground states in three dimensions

GIULIANO LAZZARONI[†]

*Dipartimento di Matematica e Applicazioni “Renato Caccioppoli”,
Università degli Studi di Napoli Federico II, Via Cintia, Monte S. Angelo, 80126 Napoli, Italy*

AND

ULISSE STEFANELLI[‡]

*Faculty of Mathematics, University of Vienna,
Oskar-Morgenstern-Platz 1, A-1090 Vienna, Austria and
Istituto di Matematica Applicata e Tecnologie Informatiche “E. Magenes” - CNR,
v. Ferrata 1, I-27100 Pavia, Italy*

[Received on ???; revised on ???]

We investigate the minimization of configurational energies of Brenner type. These include two- and three-body interaction terms which favor the alignment of first neighbors. In particular, such configurational energies arise in connection with the molecular-mechanical modeling of covalent sp -bonding in carbon.

Ground states in three dimensions are characterized and the stability of chains and rings is discussed. The interaction energy is then augmented with terms corresponding to weaker interactions favoring the stratification of configurations. This gives rise to stratified structures which are reminiscent of nanoscrolls and multi-wall nanotubes. Optimal stratified configurations are identified and their geometry is discussed.

Keywords: configurational energy; carbon; ground states; stability.

1. Introduction

Carbon forms a variety of different nanostructures, ranging from three-dimensional diamond, to two-dimensional graphene and graphite, fullerenes, and nanotubes. This rich phenomenology originates from the nature of covalent bonding in carbon, which may show either sp^3 -, sp^2 -, or sp^1 -orbital hybridization favoring specific bond angles between adjacent bonds (Clayden *et al.*, 2012; Wade, 2012). In particular, sp^3 bonding arises in diamond whereas sp^2 bonds arise in locally two-dimensional configurations like graphene and nanotubes.

A strong research activity is presently directed to *carbyne* (linear acetylenic carbon), namely a long chain of sp^1 -bonded carbon atoms (Liu *et al.*, 2013). Theoretical predictions indicate carbyne as a remarkable structure, stable up to 3000 K and having a specific strength of the order of 10^8 Nm/Kg. This makes carbyne the strongest known material, 10^5 -times stronger than conventional steel (Itzhaki *et al.*, 2005b).

The actual synthesis of carbyne chains is a very delicate technical task (Baughman, 2006) and currently drives a competition between different groups worldwide. As we write, the current record of the longest chain amounts to more than 6000 atoms and has been obtained by caging carbyne within a

[†]Email: giuliano.lazzaroni@unina.it

[‡]Corresponding author. Email: ulisse.stefanelli@univie.ac.at

double-walled carbon nanotube (Shi *et al.*, 2016). Carbyne is also known to roll-up into rings, which then may combine in a variety of carbon clusters (Jones & Seifert, 1997).

The aim of this note is to analyze locally one-dimensional, chain-like structures within the framework of Molecular Mechanics (Allinger, 2010). Carbon configurations are modeled as a collection of atoms interacting via a *configurational energy* of Brenner type (Brenner, 1990; Brenner *et al.*, 2002), see (2.1). This is given in terms of classical, mass-spring potentials and takes into account both attractive-repulsive *two-body* first-neighbor interactions, minimized at some given bond length, and *three-body* terms favoring alignment between adjacent bonds, i.e. sp^1 bonds (see also Stillinger & Weber, 1985; Tersoff, 1988). The specific assumptions on the interaction energy are introduced and discussed in Section 2.

Our first result is a complete characterization of chain-like ground states in three dimensions (Theorem 3.2). We prove that the unique (up to isometries) ground state with n atoms is a straight, uniformly spaced configuration for n small and a planar ring for n large. This pairs well with the *local minimality* analysis of the same structures from Stefanelli (2017).

We then extend the reach of the theory by addressing stratified configurations. These emerge quite naturally by the effect of weaker bonds (so called π -bonds) which operate between sp^1 - and sp^2 -bonded structures. A first example of such occurrence is *graphite*, where sp^2 platelets are bonded to form a three-dimensional structure. Other examples are *multi-wall nanotubes* (Lehman *et al.*, 2011) and *nanoscrolls* (Li *et al.*, 2009), consisting of a stratification of different locally-two-dimensional tubes. *Carbon onions* (Butenko *et al.*, 2014), namely multi-shell fullerenes, are again stratified configurations (Tománek *et al.*, 1993).

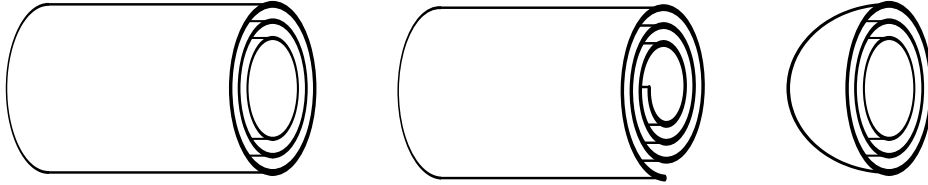


FIG. 1. Schematics of stratified carbon nanostructures as sections (bold) of a multi-wall nanotube (left), a nanoscroll (middle), and a carbon onion (right).

As a first, very schematic modelization of sections of multi-wall nanotubes, nanoscrolls, or carbon onions we focus here on stratifications of one-dimensional structures. The idea is to augment the configurational energy already introduced above for carbyne by a term favoring the stratification of atoms the same site. Details in this direction are given in Section 4. A delicate balance between bonding and stratification ensues, giving rise to specific stratified configurations. Our second main result (Theorem 4.3) identifies such stratified ground states as the number of atoms grows. As we shall see, stratified ground states are not a mere layering of multiple nonstratified ground states and stratification drives the emergence of distinguished geometries.

In order to put our work in perspective, we provide here a brief account of crystallization results for carbon nanostructures. *Global minimality* results have to be traced back to E & Li (2009), where graphene is proved to be a ground state in two dimensions: By assuming the three-body energy term to favor sp^2 bonding, the *thermodynamic limit* for a large number of particles, namely $n \rightarrow \infty$, is ascertained to correspond to a suitably compressed regular hexagonal lattice. This result corresponds to a three-body version of the seminal theory by Theil (2006) who considered Lennard-Jones-like two-body

interactions. In the context of thermodynamic limits, Farmer *et al.* (2017) recover the hexagonal lattice in the thermodynamic limit by assuming the three-body energy term to favor sp^1 bonding instead, namely in the very setting of Brenner interactions of this paper.

In the setting of *finite* crystallization, namely for the number n of atoms being finite, two-dimensional ground states of sp^2 interactions are proved to be patches of the hexagonal lattice by Mainini & Stefanelli (2014). These are generically not unique and can be characterized in terms of a discrete isoperimetric inequality (Davoli *et al.*, 2016). In particular, one can quantitatively check the emergence of a hexagonal Wulff shape as the number of atoms increases.

This paper delivers, to our knowledge, the first crystallization results based on global minimization in three dimensions for a *finite* number of atoms. Proving finite crystallization in three dimensions is a daunting task, for all of the available techniques hinge on lower dimensional concepts (De Luca & Friesecke, 2017; Radin, 1981). The results of this paper are no exception, since we also use lower dimensional properties, specifically convexity and planarity, and succeed in taming three-dimensionality by exploiting the essentially one-dimensional nature of the objects in study.

Let us however mention that some three-dimensional crystallization result in the *thermodynamic limit case* $n \rightarrow \infty$ is already available. Specifically, Sütő (2005, 2006) discusses the emergence of periodic and aperiodic infinite-volume ground state configurations for some specific class of pair interaction potentials, and Flatley & Theil (2015) prove the minimality of the *face-centered cubic* lattice under Lennard-Jones-type interactions.

As for *local minimality (stability)* one has to record the convexity argument by Mainini & Stefanelli (2014), which allows checking the two fullerenes C_{20} and C_{60} are stable. These ideas have then been extended by Stefanelli (2017), where the stability of corannulene, diamond, and lonsdaleite is also addressed. Local minimality is also employed as a selection criterion among different carbon-nanotube and fullerene geometries by Friedrich *et al.* (2016), Mainini *et al.* (2017a,b), also in relation with their behavior under traction. The literature here is vast and we limit ourselves in mentioning some contributions (Arroyo & Belytschko, 2005; Favata & Podio-Guidugli, 2015; Yakobson *et al.*, 1996) among many others. Kass & Monneau (2014) proved a Saint Venant principle under long-range, purely two-body interactions. The Cauchy-Born hypothesis for carbon nanotubes under traction is rigorously validated in the sp^2 case (Friedrich *et al.*, 2017); see also Mainini *et al.* (2017a) for some numerical evidence. As for the modelization of stratified carbon configurations, the reader is referred to Golovaty & Talbott (2008) where a continuum model accounting for the *polygonalization* effect in multi-walled nanotubes is investigated. This has indeed been modeled via one-dimensional chains in the plane by Nixdorf (2014). A rigorous discrete-to-continuum theory relating planar chains to the Elastica Functional was provided by Español *et al.* (2018).

2. Configurational energy

As mentioned in the Introduction, we model carbon configurations within the frame of Molecular Mechanics (Allinger, 2010) by identifying them with the positions of the nuclei, namely with collections of points in the three-dimensional space. To all configurations $X = \{x_1, \dots, x_n\}$ of n atoms in \mathbb{R}^3 we associate a *configurational energy* $E : \mathbb{R}^{3n} \rightarrow \mathbb{R} \cup \{\infty\}$ given by

$$E(X) = E_2(X) + E_3(X) := \frac{1}{2} \sum_{i \neq j} v_2(|x_i - x_j|) + \frac{1}{2} \sum_{(i,j,k) \in T} v_3(\theta_{ijk}), \quad (2.1)$$

modeled on the sp -covalent bonds in carbon (Clayden *et al.*, 2012). This results in what is usually referred to as *Brenner-like* potential (Brenner, 1990; Farmer *et al.*, 2017). The configurational energy E

is the sum of a *two-body* term E_2 , depending solely on the mutual distance of the atoms, and a *three-body* contribution E_3 , depending on bond angles instead (see below). The lower semicontinuous two-body interaction density $v_2 : [0, \infty) \rightarrow \mathbb{R} \cup \{\infty\}$ is assumed to be of attractive-repulsive type and short-ranged. In particular, we ask for

$$-1 = v_2(1) < v_2(r) \quad \forall r \neq 1, \quad (2.2)$$

$$v_2(r) = \infty \quad \forall r < 1 - \varepsilon, \quad (2.3)$$

$$v_2(r) = 0 \quad \forall r > 1 + \varepsilon \quad (2.4)$$

where $\varepsilon > 0$ is some given small parameter. Condition (2.2) expresses the fact that atomic bonds have a preferential bond length, here normalized to 1. This is clearly an idealization, since bond lengths are heavily depending on chemistry and geometry.

Assumption (2.3) corresponds to atomic repulsion: no pair of atoms can be closer than $1 - \varepsilon$. Correspondingly, condition (2.4) expresses the fact that interactions are short-ranged (see below). We say that the two atoms x_i and x_j are *bonded* or that there exists a *bond* between x_i and x_j iff $1 - \varepsilon < |x_i - x_j| < 1 + \varepsilon$. To all configurations we associate the respective *bond graph* resulting from taking the atomic positions as vertices and the existing bonds as edges, represented as straight segments. Note that such segments cannot cross each other if ε is chosen to be small enough.

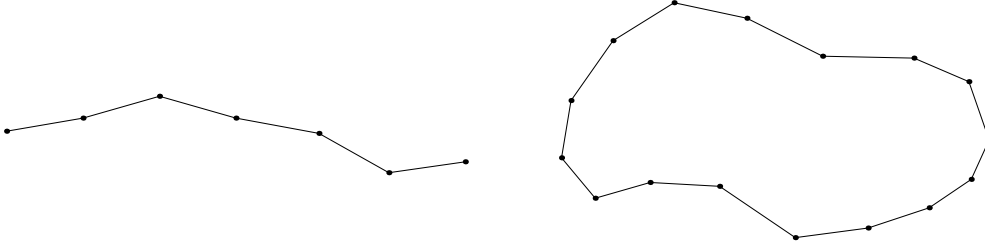


FIG. 2. Configurations and their bond graph.

In the following we specify the indexes corresponding to bonded atoms (first neighbors) as

$$N = \{(i, j) \in \{1, \dots, n\} \times \{1, \dots, n\} : 1 - \varepsilon < |x_i - x_j| < 1 + \varepsilon\}.$$

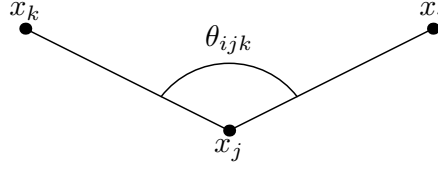
Note that $(i, j) \in N$ iff $(j, i) \in N$, so that all bonds are counted twice in N . This motivates the occurrence of the factor $1/2$ in the definition of E_2 . Assumptions (2.3)-(2.4) entail that indeed the sum in E_2 can be equivalently restricted to pairs $(i, j) \in N$, whenever E_2 is finite.

The three-body interaction energy E_3 is responsible for the topology of the bond graph and it is modulated by the *three-body* interaction density $v_3 : [0, \pi] \rightarrow [0, \infty)$. This is assumed to be lower semicontinuous, twice-differentiable at π , and such that

$$0 = v_3(\pi) < v_3(\theta) \quad \forall \theta \neq \pi, \quad v_3'(\pi) = 0, \quad (2.5)$$

favoring indeed angles of amplitude π . The angle θ_{ijk} in the definition of E is the angle formed by the segments (x_i, x_j) and (x_k, x_j) that is not greater than π , see Figure 3. The index set T is defined as

$$T = \{(i, j, k) : (i, j) \in N, (j, k) \in N, i \neq k\}.$$

FIG. 3. The bond angle θ_{ijk} .

Note that $(i, j, k) \in T$ iff $(k, j, i) \in T$, so that bond angles are counted twice in the sum defining E_3 . This motivates the occurrence of the factor $1/2$ in front of such sum. Under the above provisions, the energy E turns out to be invariant upon relabeling of the atoms.

Assumption (2.5) favors bond angles of amplitude π . Still, some quantification is needed in order to give rise to chain-like minimizers (note that in the extremal case $v_3 = 0$ ground states are subsets of the triangular lattice in two dimensions (De Luca & Friesecke, 2017; Heitman & Radin, 1980; Radin, 1981; Wagner, 1983)). We hence assume three-body interactions to be strong enough to determine the local one-dimensional topology of the ground-state bond graph. In particular, we ask that

$$\begin{aligned} &\text{each atom of a ground state has at most two neighbors and} \\ &\text{all bond angles are at least } \theta_{\min} \in (0, \pi). \end{aligned} \tag{2.6}$$

This happens to be the case if v_3 is large enough in parts of its domain. We present here a sufficient condition in this direction.

PROPOSITION 2.1 (Local one-dimensional geometry) Under assumptions (2.2)-(2.5) condition (2.6) follows for ε small and $v_3 > 12$ on $(0, 2\pi/3]$.

Proof. As the *kissing number* (i.e., the maximal number of disjoint unit spheres that are tangent to a given unit sphere) in three dimensions is 12 (Conway & Sloane, 1999), we start by noting that the parameter ε can be chosen so small that each ground-state atom has at most 12 neighbors. In order to check this, one has to consider a slight variant of the kissing problem, where the central sphere has radius $1 + \varepsilon$ and the touching spheres have the smaller radius $1 - \varepsilon$. We claim that, for small ε , the kissing number k_ε for the case of spheres with different radii $1 + \varepsilon$ and $1 - \varepsilon$ is still 12. This follows by a continuity argument. Assume this to be not the case and center the central sphere in $0 \in \mathbb{R}^3$. Then, for all $\varepsilon > 0$ one can find at least 13 centers of small spheres $x_\varepsilon^i \in \mathbb{R}^3$, $i = 1, \dots, 13$ with the following properties

$$|x_\varepsilon^i| = 2, \quad |x_\varepsilon^i - x_\varepsilon^j| \geq 2 - 2\varepsilon \quad \forall i, j = 1, \dots, 13, i \neq j.$$

By extracting some nonrelabeled subsequences we pass to the limit $x_\varepsilon^i \rightarrow x_0^i$ where

$$|x_0^i| = 2, \quad |x_0^i - x_0^j| \geq 2 \quad \forall i, j = 1, \dots, 13, i \neq j.$$

This yields that $k_0 \geq 13$, which is clearly false.

Assume now by contradiction that the ground-state atom x_j has three neighbors x_i, x_k, x_ℓ . Then, one of the bond angles θ_{ijk} , $\theta_{ij\ell}$, and $\theta_{kj\ell}$ is at most $2\pi/3$. (Indeed, if both θ_{ijk} and $\theta_{ij\ell}$ are larger than $2\pi/3$, then $\theta_{kj\ell}$ is maximized when all atoms x_j, x_i, x_k, x_ℓ are coplanar and $\theta_{ijk} + \theta_{ij\ell} + \theta_{kj\ell} = 2\pi$.) By removing x_j from the configuration (that is, by considering another configuration where the atom originally in x_j is displaced in such a way that it has no neighbors), the angle energy is reduced by at

least by $v_3(\theta_{ijk}) + v_3(\theta_{ijl}) + v_3(\theta_{kjl}) > 12$ and at most 12 bonds are broken. This entails an overall energy drop, contradicting minimality.

As all bonds range between $1 - \varepsilon$ and $1 + \varepsilon$, bond angles are necessarily larger than the smallest angle of a triangle with two sides of length $1 + \varepsilon$ and one side of length $1 - \varepsilon$. One hence defines $\theta_{\min} = 2 \arcsin((1 - \varepsilon)/(2(1 + \varepsilon))) < \pi/3$. Note that $\theta_{\min} \rightarrow \pi/3$ as $\varepsilon \rightarrow 0$. \square

As the energy E is invariant by translation and rotation, we shall tacitly assume that all statements in the following are meant up to isometries.

3. Ground states

Condition (2.6) prescribes the local one-dimensional structure of ground states. Let us hence starting by checking that ground states actually exist.

PROPOSITION 3.1 (Ground states exist) E admits a minimizer.

Proof. Let X_k be an infimizing sequence of configurations with $\#X_k = n$. Any connected component of the bond graph of X_k contains at most n atoms and is hence contained in ball of radius $(1 + \varepsilon)n$ by (2.6). (Note that we will prove in Theorem 3.2 below that ground states are connected.) As the connected components of X_k are at most n , by possibly translating them one can find another sequence of configurations \tilde{X}_k with the same energy $E(\tilde{X}_k) = E(X_k)$ which is contained in a ball of radius $(1 + \varepsilon)n^2$. The configurations \tilde{X}_k are hence contained in a compact set of \mathbb{R}^{3n} and one can extract some nonrelabeled subsequence $\tilde{X}_k \rightarrow X$. The lower semicontinuity of v_2 and v_3 entail that $\inf E = \lim_{k \rightarrow \infty} E(\tilde{X}_k) \geq E(X)$. This proves that X minimizes E . \square

The focus of this section is on the characterization of the global geometry of ground states. To this aim, we introduce a further assumption on the three-body interaction density, namely,

$$v_3 \text{ is strictly convex and decreasing in } (\theta_{\min}, \pi]. \quad (3.1)$$

Note that condition (3.1) follows if v_3 is C^2 in a neighborhood of π and $v_3''(\pi) > 0$.

Assumptions (2.2)-(3.1) will be considered throughout the rest of the paper, without further mentioning. The main result of this section is the following.

THEOREM 3.2 (Ground states) We have the following

- (line) If $1 < nv_3(\pi - 2\pi/n)$ the configuration

$$L_n := \{(k, 0, 0) : k = 1, \dots, n\}$$

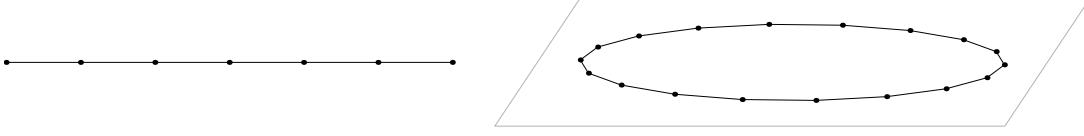
is the unique ground state.

- (ring) If $1 > nv_3(\pi - 2\pi/n)$ the configuration

$$R_n := r\{(\cos(2\pi k/n), \sin(2\pi k/n), 0) : k = 1, \dots, n\}$$

with $r = 1/(2 \sin(\pi/n))$ is the unique ground state.

In case $1 = nv_3(\pi - 2\pi/n)$ the ground states are L_n and R_n .

FIG. 4. Configurations L_7 (left) and R_{18} (right).

Proof. Let X be a ground state with connected bond graph and assume that all atoms in X have exactly two neighbors. The bond graph of X is necessarily a closed polygon (possibly not planar). In case the bond graph is homeomorphic to a circle, by indicating with θ_i the bond angle in x_i we have that

$$\begin{aligned} E(X) &\stackrel{(a)}{\geq} -n + \sum_{i=1}^n v_3(\theta_i) \stackrel{(b)}{\geq} -n + n v_3\left(\frac{1}{n} \sum_{i=1}^n \theta_i\right) \\ &\stackrel{(c)}{\geq} -n + n v_3(\pi - 2\pi/n) \stackrel{(d)}{=} E(R_n). \end{aligned}$$

We have here used that X has exactly n bonds, each contributing at least -1 to the energy (a), all bond angles are in $(\theta_{\min}, \pi]$ and v_3 is convex on the same interval (b), the sum of all bond angles being necessarily at most $\pi(n-2)$, the mean of the bond angles is at most $\pi - 2\pi/n \in (\theta_{\min}, \pi)$ and v_3 is decreasing in the same interval (c), and that the value on the left of the last equality is exactly the energy of $E(R_n)$ (d). Note that the chain of inequalities is strict whenever a bond in X has length different from 1 (a), not all bond angles are equal (b), or X is not planar (c). In particular, R_n is the unique ground state within the class of configurations whose bond graph is homeomorphic to a circle.

Let now the bond graph of X be a connected, closed polygon, not homeomorphic to a circle (knotted). Then, the Fáry-Milnor Theorem (Milnor, 1950; Sullivan, 2008) ensures that the total curvature $\sum_{i=1}^n (\pi - \theta_i)$ of the bond graph is at least 4π (recall that $\theta_i \leq \pi$). This in particular entails that

$$\frac{1}{n} \sum_{i=1}^n \theta_i \leq \pi - \frac{4\pi}{n}.$$

By arguing as above we deduce that

$$E(X) \geq -n + n v_3(\pi - 4\pi/n) > -n + n v_3(\pi - 2\pi/n) = E(R_n).$$

The energy $E(R_n)$ is hence strictly bounding from below that of any configuration whose bond graph is a closed polygon.

We now turn to the case of ground states whose bond graph is connected but is not a closed polygon. In this case the bond graph of X is necessarily homeomorphic to that of L_n . We hence have

$$E(X) \geq -n + 1 = E(L_n),$$

the inequality being strict whenever a bond in X has length different from 1 or a bond angle is different from π . The set L_n is hence the unique ground state among configurations whose bond graph is not a closed polygon.

Depending on the given n , by directly comparing the values $E(R_n)$ and $E(L_n)$ we obtain the assertion for each ground state X with connected bond graph.

It is now easy to prove that all ground states have a connected bond graph. Indeed, by arguing as above on all connected components of (the bond graph of) X one finds a collection of subconfigurations, either isomorphic to R_m or to L_m . If the bond graph of X were not connected, it would contain R_m and $R_{m'}$, or R_m and $L_{m'}$, or L_m and $L_{m'}$ and one could strictly decrease the energy by replacing them with $R_{m+m'}$, $R_{m+m'}$, or $L_{m+m'}$, respectively. \square

Theorem 3.2 states that the only ground state for large n is R_n , namely a planar, circular configuration with interatomic distance 1. This would correspond to a large carbon ring.

A straight carbyne chain L_n is not globally minimizing for large n . It is however a strict local minimizer of the energy. Indeed, let \tilde{L}_n be a small perturbation of L_n , so that the topology of the bond graph is preserved. Then $E(\tilde{L}_n) \geq -n + 1 = E(L_n)$, the inequality being strict whenever a bond in \tilde{L}_n has length different from 1 or a bond angle is different from π (that is, whenever $\tilde{L}_n \neq L_n$). The failure of global minimality for large n and the persistence of local minimality for all n correspond, although to a schematic extent, to the current understanding of carbyne. On the one hand, to produce very long carbyne chains is a very delicate task (Shi *et al.*, 2016). On the other hand, carbyne is predicted to be thermally stable at comparably high temperatures (locally minimizing) (Liu *et al.*, 2013).

4. Stratified ground states

We now turn to a modelization of stratified ground states. As mentioned in the Introduction, configurations like multi-walled nanotubes, nanoscrolls, and carbon onions can be visualized as stratifications of locally-two-dimensional, sp^2 -bonded structures (Butenko *et al.*, 2014; Lehman *et al.*, 2011; Li *et al.*, 2009). Their axial sections appear then as stratifications of one-dimensional configurations, see Figure 5. We hence extend the reach of our model by allowing configurations admitting multiple layers of atoms.

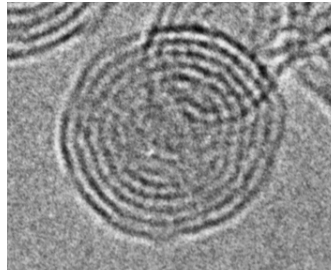


FIG. 5. A section of a carbon onion. The diameter of the structure is of the order of 5 nm and the outer layer contains roughly 120 atoms. Courtesy of S. Tomita, M. Fujii, and S. Hayashi (Tomita *et al.*, 2002).

Layers of stratified carbon configurations usually contain a different number of atoms, which occupy distinct positions in space, and stratification occurs as effect of the realization of the weaker so-called π -bonds between different layers. Aiming at mathematical tractability, we perform here a radical simplification and assume that all layers occupy the same position in space. We associate to each layer a configurational energy of the form of Section 2, namely by modeling the section of the sp^2 -bonded structure as an effective sp^1 chain. Stratification is taken into account by augmenting the energy by a term favoring interlayer interactions, that is having more atoms at the same site, see (4.1).

Let us remark that a more realistic modeling of stratified carbon nanostructures would require to deal with the actual sp^2 nature of layers, which indeed influences the fine geometries of sections, as well

as allowing atoms to occupy distinct positions in different layers. Such extensions cannot be directly accommodated within the simplified frame of our analysis, which nevertheless replicates some of the basic features of the stratification phenomenon.

4.1 Stratified energy

We assume the number n of atoms of configurations to be fixed throughout this section and indicate *stratified configurations* by the pair (X, S) where $X = (x_1, \dots, x_m) \in \mathbb{R}^{3m}$ identify atomic positions, with m varying between 1 and n , and $S = (s_1, \dots, s_m) \in \mathbb{N}^m$ with $s_1 + \dots + s_m = n$, $s_i \neq 0$, indicate layer occupancy. In particular, s_i is the number of atoms stratified at site x_i , see Figure 6. We use the notation $\lfloor y \rfloor = \min\{z \in \mathbb{Z} : y \leq z\}$ and $\lceil y \rceil = \max\{z \in \mathbb{Z} : z \leq y\}$ for $y \in \mathbb{R}$.

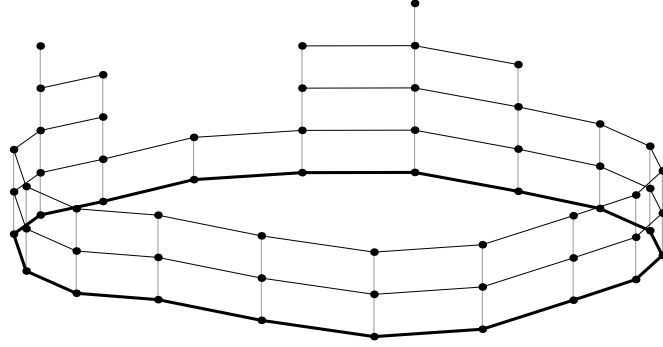


FIG. 6. A stratified configuration (X, S) . The bond graph of X is depicted in bold and the occupancy of the sites is represented by columns of atoms in the vertical direction.

The *stratified configurational energy* $E_s : \mathbb{R}^{3m} \times \mathbb{N}^m \rightarrow \mathbb{R} \cup \{\infty\}$ is defined as

$$E_s(X, S) = \frac{1}{2} \sum_{i \neq j} v_2(|x_i - x_j|) s_i \wedge s_j + \frac{1}{2} \sum_{(i,j,k) \in T} v_3(\theta_{ijk}) s_i \wedge s_j \wedge s_k - \ell n + \ell m. \quad (4.1)$$

In this formula, the occurrence of the minimum values $s_i \wedge s_j$ and $s_i \wedge s_j \wedge s_k$ entails that the terms are counted once for each layer where all corresponding atoms are present. The small parameter $\ell \in (0, 1)$ indicates the energy contribution due to interlayer interactions. In the case of carbon, this corresponds to the energy of the π -bond and is much smaller than that of sp -covalent bonds. This motivates the position $\ell < 1$ above.

For illustration, note that $E_s(X, S) = E(X)$ whenever $m = n$, that is whenever the stratified configuration actually consists of a single layer, namely $S = (1, \dots, 1)$. In case $S = (2, \dots, 2)$, that is if (X, S) consists in the stratification of two copies of X , so $n = 2m$, one deduces that

$$E_s(X, S) = 2E(X) - \ell m$$

and the stratified energy is the sum of the configurational energy of each layer and the interlayer-interaction contribution $-\ell$ for each site.

If $\ell = 0$ Theorem 3.2 ensures that the stratified ground states (X, S) of the stratified energy E_s have indeed one single layer so that X is a ground state of the energy E . On the other hand, for each $\ell > 0$

stratified ground states with large n necessarily have more layers. Let for instance $n = 2m$. Then

$$\begin{aligned} E_s(R_n, (1, \dots, 1)) &= -2m + 2mv_3(\pi - \pi/m) \\ &> -2m + 2mv_3(\pi - 2\pi/m) - \ell m \\ &= E_s(R_m, (2, \dots, 2)) \end{aligned}$$

where the inequality holds for $n = 2m$ large enough, as $v_3(\theta) \rightarrow 0$ for $\theta \rightarrow \pi$.

Let us remark that stratified ground states actually exist. Indeed, for all given $S = \{s_1, \dots, s_m\} \in N^m$ with $s_1 + \dots + s_m = n$ one can argue as in Proposition 3.1 and prove that there exists a configuration X_S minimizing $E_s(\cdot, S)$. The existence of a stratified ground state follows then from the finite minimization $\min_S E(X_S, S)$.

4.2 Cronuts

From here on, given a stratified configuration (X, S) we shall assume with no loss of generality that the labeling of $X = \{x_1, \dots, x_m\}$ is such that the first neighbors of x_i belong to the set $\{x_{(i-1) \bmod m}, x_{(i+1) \bmod m}\}$. (There may be less than two neighbors, e.g. when the graph is disconnected or homeomorphic to a line.) Here, for all $z \in \mathbb{Z}$ and $m \in \mathbb{N}$ we let $z \bmod m = p \in \{1, \dots, m\}$ iff $z - p$ is a multiple of m . Our attention will be focused on a specific subclass of stratified configurations, see Figure 7.

DEFINITION 4.1 (Cronut) We say that the stratified configuration (X, S) is a *cronut* if, by letting $p = n \bmod m$, $S = (s_1, \dots, s_m)$ is given by

$$S_m = (\lfloor n/m \rfloor, \dots, \lfloor n/m \rfloor) + \underbrace{(1, \dots, 1, 0, \dots, 0)}_{p \text{ times}}. \quad (4.2)$$

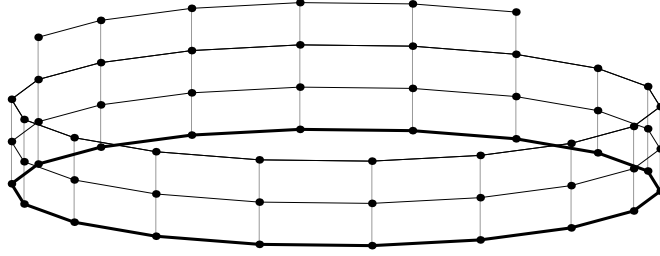


FIG. 7. A cronut.

A cronut consists of $w = \lfloor n/m \rfloor$ copies of X , plus possibly p extra atoms in a last, incomplete layer whose bond graph is homeomorphic to that of L_p (and empty if $p = 0$). As already mentioned, such configurations are reminiscent of the geometry of section of stratified carbon nanostructures, see Figure 1. Within this analogy, multi-walled carbon nanotubes and carbon onions are described by cronuts with $p = 0$. On the other hand, $p \neq 0$ would correspond to the case of the nanoscroll. More precisely, let us point out that the section of a nanoscroll can be visualized as a single chain of n atoms winding up r complete times. For the purpose of mathematical simplicity, we model this situation as r copies of ring-like configurations with m atoms each, plus a last incomplete layer of $p = n - rm$ atoms. By referring to Figure 8, let us however note this simplification preserves both the number of bonds (within the same

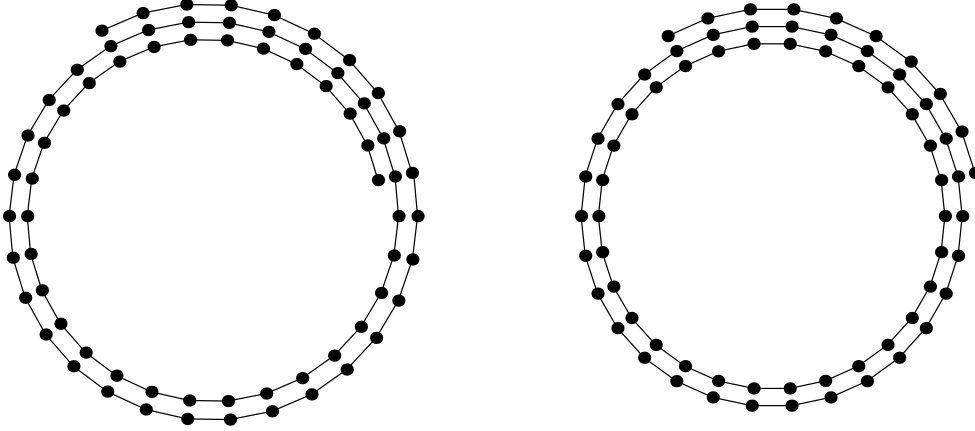


FIG. 8. The modelization of the section of a nanoscroll (left) as a cronut (right). Corresponding atoms on different layers are indeed modeled as if occupying the same position in space, see Figure 7.

layer) and π -bonds (across layers). Indeed, the two configurations in Figure 8 cannot be distinguished without taking into account the actually distinct positioning of π -bonded atoms, a higher-order effect which is neglected by our simplified approach. To conclude, note that the stratified configuration in Figure 6 is not a cronut.

Before moving on, let us present the expressions of the stratified energies of a cronut in case $X = L_m$ or $X = R_m$. We have the following:

$$E_s(L_m, S_m) = \begin{cases} -(1+\ell)n + \lfloor n/m \rfloor + \ell m & \text{if } p = 0, \\ -(1+\ell)n + \lfloor n/m \rfloor + \ell m + 1 & \text{if } p \neq 0 \end{cases} \quad (4.3)$$

and

$$E_s(R_m, S_m) = \begin{cases} -(1+\ell)n + \ell m + nv_3(\pi - 2\pi/m) & \text{if } p = 0, \\ -(1+\ell)n + \ell m + (n-2)v_3(\pi - 2\pi/m) + 1 & \text{if } p \neq 0. \end{cases} \quad (4.4)$$

Moving from the latter relation one easily gets that, given n , the optimal m for $E_s(R_m, S_m)$ scales like $n^{1/3}$ so that

$$E_s(R_m, S_m) \sim -(1+\ell)n + cn^{1/3} \text{ as } n \rightarrow \infty. \quad (4.5)$$

Here and in the following, we use the short-hand notation $a_n \sim cb_n$ in order to indicate that the two sequences a_n and b_n are of the same order as $n \rightarrow \infty$, namely that $a_n = O(b_n)$ and $b_n = O(a_n)$ as $n \rightarrow \infty$. Analogously, we write $a_n \lesssim cb_n$ if $a_n \leq O(b_n)$ as $n \rightarrow \infty$.

4.3 Optimal cronuts.

We firstly focus on the minimization of the stratified energy E_s restricted to the subclass of cronuts. Moving from this, we will consider all stratified configurations with connected bond graph in Theorem 4.3 below. We prove the following.

PROPOSITION 4.2 (Optimal cronuts) Let n be large and (X, S) be an optimal cronut with n atoms. Then, the bond graph of X is homeomorphic to a circle and $X = R_m$ iff $p \leq 2$.

Proof. Let $m = \#X$. If the bond graph X is homeomorphic to L_m , then necessarily $X = L_m$ for the latter has $E_2(L_m) = -(m-1)$ and $E_3(L_m) = 0$, both being optimal. In this case, we deduce from (4.3) that the stratified energy scales like $E_s(L_m, S) \sim -(1+\ell)n + cn^{1/2}$ as $n \rightarrow \infty$. This is however suboptimal with respect to (4.5). In particular, we have that the bond graph X is not homeomorphic to L_m for large n .

If $p = 0$ or $p = 1$ the stratified energy simply reads

$$E_s(X, S) = \lfloor n/m \rfloor E(X) - \ell n + \ell m,$$

so that the optimal cronut (X, S) is such that X minimizes E among the configurations X' with $\#X' = m$. As we already proved that $X = L_m$ is not optimal for large n , Theorem 3.2 entails that $X = R_m$. The same holds for $p = 2$ where the latter expression for E_s is just augmented by $v_2(|x_2 - x_1|)$ and $X = R_m$ minimizes both terms $v_2(|x_2 - x_1|)$ and $E_s(X, S) - v_2(|x_2 - x_1|)$.

The case $p \geq 3$ is more involved, for the bending of the last, incomplete layer of (X, S) actually affects the geometry of the configuration X , see Figure 9.

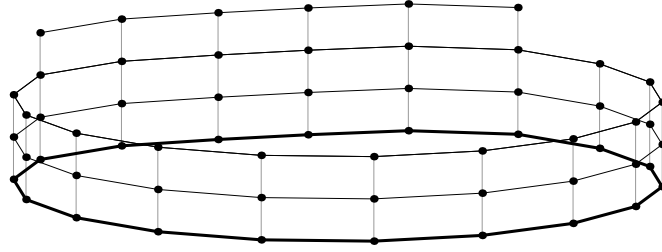


FIG. 9. In case $p \geq 3$, the optimal cronut (X, S) does not correspond to (R_m, S) from g 7. Bond angles corresponding to those atoms in the last incomplete layer having two neighbors are closer to π .

Let us check first that the bond graph of X is homeomorphic to a circle. Assume this is not the case, namely that the bond graph of X is knotted (thus $m \geq 4$). By arguing as in the proof of Theorem 3.2 we would have that $\sum_{i=1}^m (\pi - \theta_i) \geq 4\pi$ where θ_i is the bond angle at x_i . The mean of all bond angles

$$\bar{\theta} = \frac{1}{n-2} \left(\left\lfloor \frac{n}{m} \right\rfloor \sum_{i=1}^m \theta_i + \sum_{i=2}^{p-1} \theta_i \right) \quad (4.6)$$

would then fulfill

$$\begin{aligned} \bar{\theta} &\leq \pi - \frac{4\pi \lfloor n/m \rfloor}{n-2} = \pi - \frac{4\pi \lfloor n/m \rfloor}{m \lfloor n/m \rfloor + p - 2} \\ &< \pi - \frac{4\pi \lfloor n/m \rfloor}{m(\lfloor n/m \rfloor + 1)} \leq \pi - \frac{2\pi}{m} := \tilde{\theta} \end{aligned}$$

where we have used that $n = m \lfloor n/m \rfloor + p$ and $p < m$. Note that $\tilde{\theta}$ is the (internal) bond angle in R_m . In particular, by the convexity of v_3 , cf. (3.1), we would then have $E_s(X, S) > E_s(R_m, S)$ contradicting minimality.

We have hence proved that the bond graph of X is homeomorphic to a circle. Still, if $p \geq 3$ we have that $X \neq R_m$. In fact, if $X = R_m$ one could strictly lower the energy by letting all bond angles equal the mean $\bar{\theta}$ from (4.6) without changing bond lengths. This is doable (for $n \geq 4$) by making the

configuration not planar. As $X \neq R_m$, an optimal cronut does not correspond to stratified copies of the nonstratified ground state. In order to check this, let us decompose the stratified energy as

$$E_s(X, S) = -\ell n + \ell m + \left\lfloor \frac{n}{m} \right\rfloor E(X) + \sum_{i=2}^{p-1} v_3(\theta_i) + \sum_{i=2}^p v_2(|x_i - x_{i-1}|).$$

We consider now variations of the atomic positions, by keeping n and m fixed. As R_m minimizes E , the cronut (R_m, S) minimizes E_s iff the subconfiguration $\{x_1, \dots, x_p\} \subset R_m$ minimizes the last two terms above. This is however not the case, for the sum of these two terms is minimized by L_p . This proves that (R_m, S) is not a stratified ground state. \square

The round and stratified structure of the optimal cronut (X, S) for large n is reminiscent of the *cronut* pastry invented by the chef Dominique Ansel. This resemblance indeed motivated us in choosing this name.

Note that the optimal cronut is the stratification of nonstratified ground states just for $p \leq 2$. For $p > 2$ the geometry of the optimal cronut is different, although it approaches that of the nonstratified ground state as $n \rightarrow \infty$. In contrast with the nonstratified case, the optimal cronut may be nonunique (Subsection 4.4) nor have a connected bond graph (Subsection 4.7). It is remarkable that such deviations from the nonstratified-ground-state geometry may occur due to the presence of a single extra atom in the last incomplete layer, regardless of the number of the atoms in the whole configuration.

4.4 Nonuniqueness of optimal cronuts

One can find cases of nonuniqueness of optimal cronuts. An example in this direction is given by $n = q^3$ with q prime and large, $v_3(\theta) = \kappa(\pi - \theta)^2/2$ for $|\pi - \theta| \leq \pi/5$ with

$$\kappa = \frac{2\ell}{4\pi^2} \frac{q^2 - q}{q^3} \left(\frac{1}{q^2} - \frac{1}{q^4} \right)^{-1} = \frac{\ell}{2\pi^2} \frac{q^2}{q + 1}$$

by taking ℓ very small. Indeed, as κ scales with ℓ , it is a standard matter to argue as in Subsection 4.3 and check that the bond graph of X , where (X, S) is an optimal cronut, is homeomorphic to that of R_m for some m .

Note that $p = n \bmod m = 0$ iff $m = q$ or $m = q^2$ (or $m = 1$ or $m = n$, which are clearly not optimal). In this cases we can use (4.4) in order to compute that

$$E_s(R_q, (q^2, \dots, q^2)) = E_s(R_{q^2}, (q, \dots, q))$$

The value of the constant κ is specifically designed to realize this last equality.

We aim now at proving that $(R_q, (q^2, \dots, q^2))$ and $(R_{q^2}, (q, \dots, q))$ are (the only) two optimal cronuts with q^3 atoms. To this end, let (X, S) be a cronut with $m = \#X$ and assume $m \notin \{1, q, q^2, q^3\}$. Then, m does not divide q^3 and we have $p > 1$. Hence, the cronut (X, S) has at least one bond less than $(R_q, (q^2, \dots, q^2))$. In particular, the two-body part of the stratified energy of (X, S) exceeds the corresponding term of $(R_q, (q^2, \dots, q^2))$ at least by 1. By choosing ℓ small one can then induce that $E_s(X, S) > E_s(R_q, (q^2, \dots, q^2))$ so that (X, S) cannot be optimal.

The latter counterexample to uniqueness required a very specific setting. Albeit we are not in the position of offering a comprehensive discussion on uniqueness and nonuniqueness of optimal cronuts, we believe uniqueness to be generic with respect to data.

4.5 Stratified ground states are optimal cronuts

The main result of this section is a characterization of stratified ground states.

THEOREM 4.3 (Stratified ground states) For n large all stratified ground states with connected bond graph are optimal cronuts.

Proof. Let (X, S) be a stratified ground state with $m = \#X$ with a connected bond graph. Our aim is to prove that it is a cronut, therefore optimal. We subdivide the argument into steps.

Step 1: The bond graph of X is not homeomorphic to that of L_m . We argue by contradiction. Assume the bond graph of X to be homeomorphic to that of L_m . Then necessarily $X = L_m$ as the angle part of the stratified energy of L_m vanishes, therefore being optimal. In addition, one readily checks that the stratified energy is lowered by displacing atoms from the incomplete layers in order to complete lower layers, hence reducing to a cronut. From minimality we necessarily deduce that $E_s(X, S) = E_s(L_m, S_m)$ where S_m is given by (4.2).

We shall now check that m grows with n . Assume on the contrary that m stays bounded for large n . Then

$$\begin{aligned} E_s(X, S) &= E_s(L_m, S_m) \stackrel{(4.3)}{\geq} -(1+\ell)n + \lfloor n/m \rfloor + \ell m \\ &\sim -(1+\ell)n + cn \text{ as } n \rightarrow \infty \end{aligned}$$

which is not optimal, see (4.5). This proves that $m \rightarrow \infty$ as $n \rightarrow \infty$. By (4.3)-(4.4), this implies that

$$E_s(L_m, S_m) > E_s(R_m, S_m) \text{ as } n \rightarrow \infty,$$

and we conclude that (X, S) is not optimal, a contradiction.

Step 2: Upper bound on m . Recall (4.4)-(4.5) in order to get that

$$\begin{aligned} E_s(X, S) - E_s(R_m, S_m) &\gtrsim (-(1+\ell)n + \ell m) - (-(1+\ell)n + cn^{1/3}) \\ &\sim \ell m + cn^{1/3} \text{ as } n \rightarrow \infty \end{aligned}$$

where we have simply disregarded the angle part of $E_s(X, S)$. Minimality now ensures that the above right-hand side is nonpositive, namely

$$m \lesssim cn^{1/3} \text{ as } n \rightarrow \infty. \quad (4.7)$$

Step 3: Decomposition of (X, S) . Indicate with q and r the number of layers and complete layers of (X, S) , respectively, that is $q = \max s_i$ and $r = \min s_i$. Call t_j the number of atoms at layer j with $j = 1, \dots, q$. We start by rewriting

$$E_s(X, S) = E_s(X, (r, \dots, r)) + E_s(X, S - (r, \dots, r)) - \ell t_{r+1}. \quad (4.8)$$

The latter comes from *decomposing* (X, S) into two parts, of which the first one $(X, (r, \dots, r))$ contains just complete layers, and is hence a cronut, and the second one $(X, S - (r, \dots, r))$ has no complete layer. Notice that the configuration $(X, S - (r, \dots, r))$ will have some zero occupancies; the stratified energy $E(X, S - (r, \dots, r))$ does not count these as part of the number of sites of $(X, S - (r, \dots, r))$. Let $n' = n - rm$ be the number of atoms which are not in $(X, (r, \dots, r))$ and $p = n' \bmod m$.

Step 4: Lower bound on the stratified energy. Recall from Step 1 that the bond graph of X is not homeomorphic to that of L_m . In particular, one has that

$$E_s(X, (r, \dots, r)) \geq E_s(R_m, (r, \dots, r)) \quad (4.9)$$

and equality holds iff $X = R_m$.

Assume now that

$$n' > m. \quad (4.10)$$

Then, we can rearrange the atoms in $(X, S - (r, \dots, r))$ in order to complete as many layers as possible. This is achieved by changing $S - (r, \dots, r)$ into

$$S' = (\lfloor n'/m \rfloor, \dots, \lfloor n'/m \rfloor) + \underbrace{(1, \dots, 1, 0, \dots, 0)}_{p \text{ times}}$$

as we have that

$$E_s(X, S - (r, \dots, r)) \geq E_s(L_m, S - (r, \dots, r)) \geq E_s(L_m, S') \quad (4.11)$$

The first inequality above follows as no layer of $(X, S - (r, \dots, r))$ is complete so that it is better to pass to L_m as the angle part of the energy is there optimized. The second inequality is due to the fact that by changing from $(X, S - (r, \dots, r))$ to (L_m, S') one possibly activates extra bonds.

By using (4.9) and (4.11), under condition (4.10) the decomposition (4.8) delivers the strict lower bound

$$E_s(X, S) \geq E_s(R_m, (r, \dots, r)) + E_s(L_m, S') - \ell t_{r+1}. \quad (4.12)$$

Step 5: m grows with n . We have already proved that m grows with n in Step 1 under the assumption that the bond graphs of X and L_m are homeomorphic (which was then falsified). Here, we provide an argument in the general case of (4.10).

Moving from (4.12), we use relations (4.3)-(4.4) in order to quantify that

$$\begin{aligned} E_s(X, S) &> -(1+\ell)rm + rm v_3(\pi - 2\pi/m) + \ell m \\ &\quad - (1+\ell)n' + \frac{n'}{m} - 1 + \ell m - \ell t_{r+1} \\ &> -(1+\ell)n + rm v_3(\pi - 2\pi/m) + \frac{n'}{m} + \ell m - 1 \end{aligned}$$

where we have used that $t_{r+1} < m$. Assume now by contradiction that m is bounded independently of n . As $n' = n - rm$, either rm or n' is larger than $n/2$ (up to a subsequence). In case $rm \geq n/2$ one has that $rm v_3(\pi - 2\pi/m) \sim cn$ since $v_3(\pi - 2\pi/m)$ is bounded away from 0. If $n' \geq n/2$ one has that $n'/m \sim cn$. In both cases we have that

$$E_s(X, S) \sim -(1+\ell)n + cn \quad \text{as } n \rightarrow \infty$$

which is not optimal, see (4.5). We hence conclude that $m \rightarrow \infty$ as $n \rightarrow \infty$.

Step 6: Stratified ground states are cronuts. By letting n be large enough, under assumption (4.10) Step 5 ensures that m can be made so large that

$$E_s(L_m, S') > E_s(R_m, S') - \left(\left\lfloor \frac{n'}{m} \right\rfloor + 1 \right) m v_3(\pi - 2\pi/m) + \left\lfloor \frac{n'}{m} \right\rfloor \geq E_s(R_m, S'),$$

which follows as soon as m is large enough to have $2m v_3(\pi - 2\pi/m) \leq 1$, see the proof of Theorem 3.2. As we have that

$$(r, \dots, r) + S' = S_m,$$

the lower bound (4.12) yields

$$\begin{aligned} E_s(X, S) &> E_s(R_m, (r, \dots, r)) + E_s(R_m, S') - \ell t_{r+1} \\ &= E_s(R_m, S_m) + \ell m - \ell t_{r+1} > E_s(R_m, S_m) \end{aligned}$$

contradicting minimality. We hence conclude that (4.10) cannot hold, namely that $n' \leq m$. This implies that the configuration $(X, S - (r, \dots, r))$ consists, at most, of a single incomplete layer (and indeed $n' < m$). In order to conclude that the stratified ground state (X, S) is actually a cronut it hence suffices to check that the bond graph of $(X, S - (r, \dots, r))$ is connected. Indeed, assume that this is not the case and argue as follows:

$$\begin{aligned} E_s(X, S) &= E_s(X, (r, \dots, r)) + E_s(X, S - (r, \dots, r)) - \ell t_{r+1} \\ &\stackrel{(a)}{>} E(R_m, (r, \dots, r)) + E_s(L_m, S - (r, \dots, r)) - \ell t_{r+1} \\ &\stackrel{(b)}{\geq} E(R_m, (r, \dots, r)) + E_s(L_m, S') + 1 - \ell t_{r+1} \\ &\stackrel{(c)}{>} E_s(R_m, (r, \dots, r)) + E_s(R_m, S') - 2m v_3(\pi - 2\pi/m) + 1 - \ell t_{r+1} \\ &\stackrel{(d)}{>} E_s(R_m, (r, \dots, r)) + E_s(R_m, S') - \ell t_{r+1} = E_s(R_m, S'). \end{aligned}$$

Inequality (a) follows from $E_s(X, S - (r, \dots, r)) > E_s(L_m, S - (r, \dots, r))$. Then, (b) expresses the fact that, by passing from $S - (r, \dots, r)$ to S' at least one extra bond is activated, (c) uses the fact that $E_s(L_m, S') \geq E_s(R_m, S') - m v_3(\pi - 2\pi/m) + 1$, and (d) holds for $2m v_3(\pi - 2\pi/m) < 1$, namely for m large. Eventually, this proves that (X, S) is not a ground state, contradicting minimality. \square

Before moving on let us comment that, depending on the specific choice of v_3 and ℓ , for small n one could well have that E_s has a unique minimizer (L_m, S) . This is for instance the case if n is suitably small, $v_3(\theta) = k(\theta - \pi)^2$ in a suitable neighborhood of π , and k and ℓ are large enough. By focusing on the case of large n , such locally flat configurations are ruled out, see Proposition 4.2. Let us nonetheless remark that the minimizer (L_m, S) would still be an optimal cronut, in line with the statement of Theorem 4.3.

4.6 Stratified-energy scaling and aspect ratio

As checked in Proposition 4.2, for n large the optimal cronut (X, S) has a bond graph homeomorphic to a circle, still being $X \neq R_m$ if $p > 2$. On the other hand, X and R_m can be expected to come closer as n grows. In particular, we prove in the following they have the same stratified-energy asymptotics.

PROPOSITION 4.4 (Stratified-energy scaling and aspect ratio) *Stratified ground states (X, S) with n atoms and a connected bond graph fulfill*

$$\#X \sim n^{1/3} \quad \text{and} \quad E_s(X, S) \sim -(1+\ell)n + cn^{1/3} \quad \text{as } n \rightarrow \infty.$$

Proof. Let $m = \#X$. The upper bound $m \lesssim cn^{1/3}$ as $n \rightarrow \infty$ holds, see (4.7), so that we just need to check the lower bound. For $p > 2$ (the case $p \leq 2$ being analogous) we have that

$$E_s(X, S) \geq -(1+\ell)n + (n-2)v_3(\bar{\theta}) + \ell m > -(1+\ell)n + (n-2)v_3(\bar{\theta}) \quad (4.13)$$

where the first inequality follows by taking the mean of the bond angles and the second by neglecting the positive term ℓm . Owing to (4.5), minimality implies that

$$(n-2)v_3(\bar{\theta}) \lesssim cn^{1/3} \quad \text{as } n \rightarrow \infty.$$

As v_3 is twice-differentiable in π we compute that

$$\begin{aligned} cn^{-1/3} &\gtrsim \pi - \bar{\theta} = \pi - \frac{1}{n-2} \left(\left\lfloor \frac{n}{m} \right\rfloor \sum_{i=1}^m \theta_i + \sum_{i=2}^{p-1} \theta_i \right) \\ &\geq \pi - \frac{1}{n-2} \left(\left\lfloor \frac{n}{m} \right\rfloor \pi(m-2) + \pi(p-2) \right) = \frac{2\pi \lfloor n/m \rfloor}{n-2} \quad \text{as } n \rightarrow \infty, \end{aligned} \quad (4.14)$$

where we also used $\sum_{i=1}^m \theta_i \leq \pi(m-2)$ and $\theta_i \leq \pi$. The lower bound $m \gtrsim cn^{1/3}$ as $n \rightarrow \infty$ ensues.

We now derive the scaling of the stratified energy from that of m . Indeed, the upper bound $E_s(X, S) \lesssim -(1+\ell)n + cn^{1/3}$ as $n \rightarrow \infty$ has already been proved, see (4.5). On the other hand, relation (4.13) gives

$$\begin{aligned} E_s(X, S) + (1+\ell)n &\geq (n-2)v_3(\bar{\theta}) \sim c(n-2)(\pi - \bar{\theta})^2 \\ &\stackrel{(4.14)}{\sim} c(n-2) \left(\frac{2\pi \lfloor n/m \rfloor}{n-2} \right)^2 \sim cn^{1/3} \quad \text{as } n \rightarrow \infty \end{aligned}$$

where the last equivalence follows from $m \sim cn^{1/3}$ as $n \rightarrow \infty$. \square

The aspect ratio of the stratified ground state is hence dependent on the number of atoms. For larger values of n the stratified ground state has radius $cn^{1/3}$ and saturates $cn^{2/3}$ layers.

4.7 Connectedness

Differently from the nonstratified situation of Theorem 3.2, the connectedness assumption cannot be removed from the statement of Theorem 4.3. On the one hand, we believe ground states to have a connected bond graph for *most* choices of v_3 , ℓ , and n . In fact, one can prove the following.

PROPOSITION 4.5 Let (X_1, S_1) and (X_2, S_2) be optimal cronuts. If $p_1, p_2 \neq 0$ and $\#X_1$ and $\#X_2$ are large enough the union of the two optimal cronuts is not a ground state.

Proof. Denote by $n_i = \#(X_i, S_i)$, $m_i = \#X_i$, $r_i = \lfloor n_i/m_i \rfloor$ for $i = 1, 2$, and assume with no loss of generality that $m_1 \geq m_2$. The idea of the proof is rather straightforward: by detaching the last, incomplete layer of (X_2, S_2) and attaching it to the atoms on the last layer of (X_1, S_1) one activates an extra bond and the energy drops, contradicting minimality.

This is readily checked if $p_1 = p_2 = 1$, for, in this case, one has that

$$E_s(X_1, S_1) + E_s(X_2, S_2) = E_s(X_1, S_1 + (0, 1, 0, \dots, 0)) + E_s(X_2, S_2 - (1, 0, \dots, 0)) + 1.$$

The analysis of the case $p_1 > 1$ or $p_2 > 1$ is more involved. The displacement of the atoms of the last layers makes the cronuts not optimal, for the optimal geometry of the basis configuration depends on the number of atoms on the last layer, when this contains more than three atoms. We distinguish two cases, namely $p_1 + p_2 < m_1$ and $p_1 + p_2 \geq m_1$.

Assume $p_1 + p_2 < m_1$ and displace all the p_2 atoms on the last layer of (X_2, S_2) to the last layer of

(X_1, S_1) by activating an extra bond. We have that

$$\begin{aligned}
& E_s(X_1, S_1) + E_s(X_2, S_2) \\
& \geq E_s(R_{m_1}, (r_1, \dots, r_1)) + E(L_{p_1}) + E_s(R_{m_2}, (r_2, \dots, r_2)) + E(L_{p_2}) + \ell(p_1 + p_2) \\
& = E_s(R_{m_1}, (r_1, \dots, r_1)) + E(L_{p_1+p_2}) + E_s(R_{m_2}, (r_2, \dots, r_2)) + 1 + \ell(p_1 + p_2) \\
& > E_s(R_{m_1}, (r_1, \dots, r_1)) + \underbrace{(1, \dots, 1, 0, \dots, 0)}_{p_1+p_2 \text{ times}} + E_s(R_{m_2}, (r_2, \dots, r_2)),
\end{aligned}$$

where the last inequality follows from $(p_1 + p_2 - 2)v_3(\pi - 2\pi/m_1) < 1$, which holds for m_1 large. This shows that the union of the two cronuts is not a ground state.

In case $m_1 \leq p_1 + p_2$ one displaces $m_1 - p_1 \leq p_2$ atoms of the last layer of (X_2, S_2) to that of (X_1, S_1) , thus completing it. One finds

$$\begin{aligned}
& E_s(X_1, S_1) + E_s(X_2, S_2) \\
& \geq E_s(R_{m_1}, (r_1, \dots, r_1)) + E(L_{p_1}) + E_s(R_{m_2}, (r_2, \dots, r_2)) + E(L_{p_2}) + \ell(p_1 + p_2) \\
& \geq E_s(R_{m_1}, (r_1, \dots, r_1)) + E(L_{p_1}) + E_s(R_{m_2}, (r_2, \dots, r_2)) \\
& \quad + E(L_{m_1-p_1}) + E(L_{p_2-(m_1-p_1)}) - 1 + \ell(p_1 + p_2) \\
& = E_s(R_{m_1}, (r_1, \dots, r_1)) + E(L_{m_1}) + E_s(R_{m_2}, (r_2, \dots, r_2)) \\
& \quad + E(L_{p_2-(m_1-p_1)}) + \ell m_1 + \ell(p_1 + p_2 - m_1) \\
& = E_s(R_{m_1}, (r_1, \dots, r_1)) + E(R_{m_1}) + 1 - m_1 v_3(\pi - 2\pi/m_1) \\
& \quad + E_s(R_{m_2}, (r_2, \dots, r_2)) + E(L_{p_2-(m_1-p_1)}) + \ell m_1 + \ell(p_1 + p_2 - m_1) \\
& = E_s(R_{m_1}, (r_1 + 1, \dots, r_1 + 1)) + 1 - m_1 v_3(\pi - 2\pi/m_1) \\
& \quad + E_s(R_{m_2}, (r_2, \dots, r_2)) + \underbrace{(1, \dots, 1, 0, \dots, 0)}_{p_1+p_2-m_1 \text{ times}} - (p_1 + p_2 - m_1 - 2)v_3(\pi - 2\pi/m_2) \\
& > E_s(R_{m_1}, (r_1 + 1, \dots, r_1 + 1)) + E_s(R_{m_2}, (r_2, \dots, r_2)) + \underbrace{(1, \dots, 1, 0, \dots, 0)}_{p_1+p_2-m_1 \text{ times}}.
\end{aligned}$$

The last inequality holds for m_1 and m_2 large enough. Again this entails that the union of the two cronuts is not a ground state. \square

Note that the proof of Proposition 4.5 relies on the fact that $p_1 \neq 0$ and $p_2 \neq 0$. In particular, the argument does not apply to the union of two cronuts with $p_1 = p_2 = 0$. This, as we shall see now, provides a counterexample to connectedness of the bond graph. Let $n = 59$ and choose

$$v_3(\theta) = \frac{\ell}{4\pi^2}(\pi - \theta)^2 \quad \text{for } |\pi - \theta| \leq \frac{\pi}{5}$$

so that

$$v_3(\pi - 2\pi/m) = \frac{\ell}{m^2} \quad \text{for } m \geq 10.$$

As $n = 59$ is prime, for all $1 < m' < 59$ the stratified energy of a cronut can be estimated from below as

$$E_s(X_{m'}, S_{m'}) \geq -(1 + \ell)n + \ell m' + 1 \quad (4.15)$$

by simply disregarding the angle part of the energy. On the other hand, as $n = n_1 + n_2 = 20 + 39 = 2m_1 + 3m_3$ for $m_1 = 10$ and $m_2 = 13$, one could consider instead the configuration with disconnected bond graph

$$(R_{m_1}, (2, \dots, 2)) \cup (R_{m_2}, (3, \dots, 3))$$

and compute

$$\begin{aligned} & E_s((R_{m_1}, (2, \dots, 2)) \cup (R_{m_2}, (3, \dots, 3))) \\ &= E_s(R_{m_1}, (2, \dots, 2)) + E_s(R_{m_2}, (3, \dots, 3)) \\ &= -(1+\ell)n + \ell \left(m_1 + \frac{n_1}{m_1^2} \right) + \ell \left(m_2 + \frac{n_2}{m_2^2} \right) \\ &< -(1+\ell)n + \ell(23+1). \end{aligned}$$

In particular, for $\ell < 1/22$ one has that $24\ell < 2\ell + 1 \leq \ell m' + 1$ for all $1 < m' < 59$ and the configuration with disconnected bond graph has lower stratified energy with respect to the one with connected bond graph.

The key point of the latter counterexample is the fact that $n = 59$ is prime, which implies that all cronuts with n atoms and connected bond graph necessarily have $p > 0$ (excluding the nonoptimal cases $m = 1$, $m = n$). This originated the last term on the right-hand side of (4.15), which eventually allowed for the construction of a competitor with disconnected bond graph.

Acknowledgements

G.L. acknowledges the support of the Istituto Nazionale di Alta Matematica *F. Severi* and of the University of Vienna. U.S. is indebted to Alex Popov for inspiring conversations regarding the geometry of stratified ground states and acknowledges the support of the Austrian Science Fund (FWF) projects F 65, P 27052, and I 2375 and the Vienna Science and Technology Fund (WWTF) project MA14-009. The Authors would like to acknowledge the kind hospitality of the Erwin Schrödinger International Institute for Mathematics and Physics, where part of this research was developed under the frame of the Thematic Program *Nonlinear Flows*. The authors would like to thank the referees for the careful reading of the manuscript.

References

- ALLINGER, N. L. (2010) *Molecular structure: understanding steric and electronic effects from molecular mechanics*. Wiley.
- ARROYO, M. & BELYTSCHKO, T. (2005) Continuum mechanics modeling and simulation of carbon nanotubes. *Meccanica*, **40**, 455–469.
- BAUGHMAN, R. H. (2006) Dangerously seeking linear carbon. *Science*, **312**, 5776:1009–1110.
- BRENNER, D. W. (1990) Empirical potential for hydrocarbons for use in simulating the chemical vapor deposition of diamond films. *Phys. Rev. B*, **42**, 9458–9471.
- BRENNER, D. W., SHENDEROVA, O. A., HARRISON, J. A., STUART, S. J., NI, B. & SINNOTT, S. B. (2002) A second-generation reactive empirical bond order (REBO) potential energy expression for hydrocarbons. *J. Phys. Condens. Matter*, **14**, 783–802.

- BUTENKO, Y., SILLER, L. & HUNT, M. R. C. (2014) Carbon onions. *Carbon Nanomaterials* (Y. Gogotsi & V. Presser eds). CRC Press, pp. 279–302.
- CLAYDEN, J., GREEVES, N. & WARREN, S. G. (2012) *Organic chemistry*. Oxford University Press.
- CONWAY, J. H. & SLOANE, N. J. A. (1999) *Sphere Packings, Lattices and Groups*, 3rd edition. Springer-Verlag.
- DAVOLI, E., PIOVANO, P. & STEFANELLI, U. (2016) Wulff shape emergence in graphene. *Math. Models Methods Appl. Sci.*, **26**, 12:2277–2310.
- DE LUCA, L. & FRIESECKE, G. (2017) Crystallization in two dimensions and a discrete Gauss-Bonnet theorem. *J. Nonlin. Sci.*, **28**, 69–90.
- E, W. & LI, D. (2009) On the crystallization of 2D hexagonal lattices. *Comm. Math. Phys.*, **286**, 3:1099–1140.
- EL KASS, D. & MONNEAU, R. (2014) Atomic to continuum passage for nanotubes: a discrete Saint-Venant principle and error estimates. *Arch. Ration. Mech. Anal.*, **213**, 25–128.
- ESPAÑOL, M. I., GOLOVATY, D. & WILBER, J. P. (2018) Euler elastica as a Γ -limit of discrete bending energies of one-dimensional chains of atoms. *Math. Mech. Solids*, **23**, 1104–1116.
- FARMER, B., ESEDOĞLU, S. & SMEREKA, P. (2017) Crystallization for a Brenner-like potential. *Comm. Math. Phys.*, **349**, 1029–1061.
- FAVATA, A. & PODIO-GUIDUGLI, P. (2015) A shell theory for carbon nanotube of arbitrary chirality. *Shell and membrane theories in mechanics and biology*. Adv. Struct. Mater., **45**, Springer, pp. 155–167.
- FLATLEY, L. C. & THEIL, F. (2015) Face-centered cubic crystallization of atomistic configurations. *Arch. Ration. Mech. Anal.*, **218**, 363–416.
- FRIEDRICH, M., PIOVANO, P. & STEFANELLI, U. (2016) The geometry of C_{60} . *SIAM J. Appl. Math.*, **76**, 2009–2029.
- FRIEDRICH, M., MAININI, E., PIOVANO, P. & STEFANELLI, U. (2017) Characterization of optimal carbon nanotubes under stretching and validation of the Cauchy-Born rule. *Arch. Ration. Mech. Anal.*, to appear.
- GOLOVATY, D. & TALBOTT, S. (2008) Continuum model of polygonization of carbon nanotubes. *Phys. Rev. B*, **77**, 081406(R).
- HEITMAN, R. & RADIN, C. (1980) Ground states for sticky disks. *J. Stat. Phys.*, **22**, 3:281287.
- ITZHAKI, L., ALTUS, E., BASCH, H. & HOZ, S. (2005b) Harder than Diamond: Determining the Cross-Sectional Area and Young’s Modulus of Molecular Rods. *Angew. Chem. Int. Ed.*, **44**, 45:7432–7435.
- JONES, R. O. & SEIFERT, G. (1997) Structure and bonding in carbon clusters C_{14} to C_{24} : chains, rings, bowls, plates, and cages. *Phys. Rev. Lett.*, **79**, 443.

- LEHMAN, J. H., TERRONES, M., MANSFIELD, E., HURST, K.E. & MEUNIER, V. (2011) Evaluating the characteristics of multiwall carbon nanotubes. *Carbon*, **49**, 2581–2602.
- LI, Q. L. *et al.* (2009) Controlled fabrication of high-quality carbon nanoscrolls from monolayer graphene. *Nano Letters*, **9**, 2565–2570.
- LIU, M. *et al.* (2013) Carbyne from first principles: chain of C atoms, a nanorod or a nanorope. *ACS Nano*, **7**, 10075–10082.
- MAININI, E., MURAKAWA, H., PIOVANO, P. & STEFANELLI, U. (2017a) A numerical investigation on carbon nanotube geometries. *Discrete Contin. Dyn. Syst. Ser. S*, **10**, 141–160.
- MAININI, E., MURAKAWA, H., PIOVANO, P. & STEFANELLI, U. (2017b) Carbon-nanotube geometries as optimal configurations. *Multiscale Model. Simul.*, **15**, 1448–1471.
- MAININI, E. & STEFANELLI, U. (2014) Crystallization in carbon nanostructures. *Comm. Math. Phys.*, **328**, 2:545–571.
- MILNOR, J. (1950) On the curvature of knots. *Ann. of Math.*, **52**, 248–257.
- NIXDORF, T. A. (2014) A mathematical model for carbon nanoscrolls. Master Thesis, University of Akron.
- RADIN, C. (1981) The ground state for soft disks. *J. Stat. Phys.*, **26**, 2:365–373.
- SHI, L. *et al.* (2016) Confined linear carbon chains as a route to bulk carbyne. *Nature Mat.*, **15**, 634–639.
- STEFANELLI, U. (2017) Stable carbon configurations. *Boll. Unione Mat. Ital (9)*, to appear.
- SULLIVAN, J. M. (2008) Curves of finite total curvature. *Discrete differential geometry* (A. I. Bobenko, P. Schröder, J. M. Sullivan & G. M. Ziegler eds). *Oberwolfach Seminars*, **38**, 137–161.
- SÜTŐ, A. (2005) Crystalline ground states for classical particles. *Phys. Rev. Lett.*, **95**, 265501.
- SÜTŐ, A. (2006) From bcc to fcc: Interplay between oscillation long-range and repulsive short range forces. *Phys. Rev. B*, **74**, 104117.
- STILLINGER, F. H. & WEBER, T. A. (1985) Computer simulation of local order in condensed phases of silicon. *Phys. Rev. B*, **8**, 5262–5271.
- TERSOFF, J. (1988) New empirical approach for the structure and energy of covalent systems. *Phys. Rev. B*, **37**, 6991–7000.
- THEIL, F. (2006) A proof of crystallization in two dimensions. *Comm. Math. Phys.*, **262**, 1:209–236.
- TOMÁNEK, D., ZHONG, W. & KRASTEV, E. (1993) Stability of multishell fullerenes. *Phys. Rev. B*, **48**, 15461–15464.
- TOMITA, S., FUJII, M. & HAYASHI, S. (2002) Optical extinction properties of carbon onions prepared from diamond nanoparticles. *Phys. Rev. B*, **66**, 245424.
- WADE, L. G. (2012) *Organic Chemistry*, 8th edition. Pearson.

- WAGNER, H. J. (1983) Crystallinity in Two Dimensions: A Note on a Paper of C. Radin. *J. Stat. Phys.*, **33**, 3:523–526.
- YAKOBSON, B. I., BRABEC, C. J. & BERNHOLC, J. (1996) Nanomechanics of carbon tubes: instabilities beyond linear response. *Phys. Rev. Lett.*, **76**, 2511–2514.